Received: 18 December 2020 | Revised: 25 March 2021 | Accepted: 29 March 2021

DOI: 10.1111/cts.13047

ARTICLE

# Application of a PBPK model to elucidate the changes of systemic and liver exposures for rosuvastatin, carotegrast, and bromfenac followed by OATP inhibition in monkeys

**Yaofeng Cheng** | **Xiaomin Liang** | **Jia Hao** | **Congrong Niu** | **Yurong Lai**

Drug Metabolism, Gilead Sciences Inc., Foster City, CA, USA

**Correspondence**
Yurong Lai, Gilead Sciences Inc. 333 Lakeside Dr. Foster City, CA 94404, USA.
Email: Yurong.Lai@gilead.com

**Funding information**
No funding was received for this work.

## Abstract

The impact of organic anion-transporting polypeptide (OATP) inhibition on systemic and liver exposures of three OATP substrates was investigated in cynomolgus monkeys. A monkey physiologically-based pharmacokinetic (PBPK) model was constructed to describe the exposure changes followed by OATP functional attenuation. Rosuvastatin, bromfenac, and carotegrast were administered as a single intravenous cassette dose (0.5 mg/kg each) in monkeys with and without predosing with rifampin (RIF; 20 mg/kg) orally. The plasma exposure of rosuvastatin, bromfenac, carotegrast, and OATP biomarkers, coproporphyrin I (CP-I) and CP-III were increased 2.3, 2.1, 9.1, 5.4, and 8.8-fold, respectively, when compared to the vehicle group. The liver to plasma ratios of rosuvastatin and bromfenac were reduced but the liver concentration of the drugs remained unchanged by RIF treatment. The liver concentrations of carotegrast, CP-I, and CP-III were unchanged at 1 h but increased at 6 h in the RIF-treated group. The passive permeability, active uptake, and biliary excretion were characterized in suspended and sandwich-cultured monkey hepatocytes and then incorporated into the monkey PBPK model. As demonstrated by the PBPK model, the plasma exposure is increased through OATP inhibition while liver exposure is maintained by passive permeability driven from an elevated plasma level. Liver exposure is sensitive to the changes of metabolism and biliary clearances. The model further suggested the involvement of additional mechanisms for hepatic uptakes of rosuvastatin and bromfenac, and of the inhibition of biliary excretion for carotegrast, CP-I, and CP-III by RIF. Collectively, impaired OATP function would not reduce the liver exposure of its substrates in monkeys.

## Study Highlights

### WHAT IS THE CURRENT KNOWLEDGE ON THE TOPIC?

Challenges remain in understanding the impact of hepatic uptake transporter, OATPs, on plasma and liver concentrations for OATP substrate drugs with distinct pharmacokinetic (PK) profiles and elimination routes.

Cheng and Liang equally contributed to this study.

This is an open access article under the terms of the Creative Commons Attribution-NonCommercial License, which permits use, distribution and reproduction in any medium, provided the original work is properly cited and is not used for commercial purposes.
© 2021 The Authors. *Clinical and Translational Science* published by Wiley Periodicals LLC on behalf of the American Society for Clinical Pharmacology and Therapeutics.

**WHAT QUESTION DID THIS STUDY ADDRESS?**

How do hepatic active transport, metabolism, biliary excretion, and passive permeability impact the systemic and liver exposure?

**WHAT DOES THIS STUDY ADD TO OUR KNOWLEDGE?**

This study elucidates the important roles of hepatic active transport in determining drug plasma and liver concentrations and the translation of in vitro data to in vivo using the physiologically-based PK modeling approach.

**HOW MIGHT THIS CHANGE CLINICAL PHARMACOLOGY OR TRANSLATIONAL SCIENCE?**

The disconnection between plasma concentration and liver exposure followed by OATP activity reduction can explain the PK/pharmacodynamic relationship for the liver-targeted drugs.

## INTRODUCTION

The organic anion-transporting polypeptide (OATP) is a family of membrane proteins that plays a significant role in the disposition of many endogenous and exogenous substances.[1] OATP1B1 (SLCO1B1) and OATP1B3 (SLCO1B3) are the two members in the family predominantly expressing on the sinusoidal membrane of hepatocytes and are involved in taking up the body essentials and metabolic waste into liver. For example, OATP1B1/1B3 transport unconjugated and conjugated bilirubin into the liver. Loss of OATP functions caused by homozygous mutation of SLCO1B1 and SLCO1B3 genes can lead to hyperbilirubinemia, a genetic disease known as Rotor syndrome.[2] Additionally, OATP transporters facilitate the uptake of certain bile acids, such as cholic acid, chenodeoxycholic acid, and deoxycholic acid, into hepatocytes for further metabolism and contribute significantly to the bile salt enterohepatic recirculation.[3,4] Recent publications also demonstrated that OATPs transport endogenous molecules coproporphyrin I (CP-I) and CP-III, which can be used as biomarkers to monitor OATPs function.[5,6]

Many drugs are transported into the liver by OATPs and subsequentially undergo biotransformation and biliary excretion.[7] Cholesterol lowering statin drugs have been reported to be substrates of OATP1B1/1B3. Therefore, OATP-mediated hepatic uptake can be the rate limiting step of systemic clearance for statins with low passive membrane permeability. As a result, the systemic exposure of these drugs can be affected by the activity of the transporters due to either genetic variations or the presence of the inhibitors. Drugs known to be OATP1B1 substrates have shown an increased plasma exposure and reduced hepatic clearance in subjects carrying OATP1B1 *5 or *15.[8] When co-administered orally with rifampin (RIF), a known OATP pan inhibitor, the systemic exposure of pitavastatin was increased 5.7-fold in humans.[9] Similar drug-drug interactions (DDIs) have been reported for many OATP1B1/1B3 inhibitors and their substrates.[10]

Although the impact of OATP1B1/1B3 on the drug plasma exposures has been well-characterized, only a few studies have been conducted to elucidate the relationship between transporter functions and the liver exposure of their substrate drugs.[11,12] The drug concentration in the liver is determined by several processes, including passive diffusion, transporter (i.e., OATP1B1/1B3) mediated sinusoidal uptake and efflux, metabolism, and biliary excretion. Over the past a few years, limited studies revealed that OATP inhibition has a minimal impact on the liver exposure.[11] As evaluated using positron emission tomography, the total radioactivity in the liver was not significantly changed in the first 30 min following a single IV dose of $^{11}$C-rosuvastatin in subjects co-administered with an OATP inhibitor, cyclosporin A.[13] In addition to rosuvastatin, further evaluation is necessary to fully understand the impact of OATP transporter inhibition on liver exposures of other drugs with different metabolic/transport pathways.

OATP1B1 and OATP1B3 have both been identified in cynomolgus monkey and their gene sequences are 91.9% and 93.5% identical to the human orthologs.[14] In the transporter recombinantly overexpressing HEK293 cells, the ability of OATP1B1/1B3 to uptake known substrates is very similar between monkeys and humans.[15] Several other studies also indicated that the cynomolgus monkey is a good animal model to characterize OATP function.[16,17] Thus, we used the cynomolgus monkey to investigate the liver exposure of rosuvastatin, carotegrast, and bromfenac in the absence and presence of RIF, an OATP inhibitor. In this study, blood samples were collected up to 24 h and liver tissues were sampled up to 6 h post drug administration, to capture the distribution and elimination phase of pharmacokinetics (PKs) for each drug in plasma and liver. In addition, a physiologically-based PK (PBPK) model was built to incorporate factors, such as in vitro hepatic uptake,

biliary excretion, and metabolism processes for the understanding of PK changes of these three drugs in both plasma and the liver.

## MATERIALS AND METHODS

### Chemicals

Rosuvastatin, bromfenac, RIF, RIF SV, and midazolam were purchased from Sigma-Aldrich, Inc (St. Louis, MO). Carotegrast was synthesized at Gilead Sciences. CP-I and CP-III reference standards and stable isotope labeled CP-I (N4-CP-I) and CP-III (D8-CP-III) were purchased from Toronto Research Chemicals (North York, ON, Canada). Cryopreserved monkey hepatocytes (lot #UHK) were obtained from BioIVT (Hicksville, NY). All other reagents and solvents were of analytical grade.

### Pharmacokinetic study in cynomolgus monkeys

The PKs and liver exposure of intravenously dosed rosuvastatin, carotegrast, and bromfenac were characterized in cynomolgus monkeys in the presence and absence of the oral administration of OATP inhibitor, RIF, at 20 mg per kilogram body weight. The study was conducted at WuXi AppTec Co., Ltd., a contract research organization certified by the Association for Assessment and Accreditation of Laboratory Animal Care. The study protocol and experimental procedures were approved by the Institutional Animal Care and Use Committee. All animals were housed in rooms with controlled humidity (40% to 70%), temperature (18°C to 26°C), air changes (10–20 per hour), and light/dark cycle (12 h). Non-naïve male cynomolgus monkeys (3–5 kg and 2.5–6 years old) were acclimated for at least 2 weeks. Prior to the study, a physical examination for general health was conducted. All animals were then fasted overnight, and food was returned 4 h post oral dose. Water was available ad libitum throughout the whole study.

Eighteen animals were randomly assigned to two groups. Both groups received a single oral dose of either RIF or vehicle (100% PEG300) 3 h before the IV infusion (30 min) of rosuvastatin, carotegrast, and bromfenac. RIF was prepared in 100% PEG300 (20 mg/ml; dose volume of 1 ml/kg for 20 mg/kg dose). The cassette dose of rosuvastatin, carotegrast, and bromfenac was co-formulated at the final dose of 0.5 mg/kg for each testing article in 5% dextrose solution (pH 9.4, 2 ml/kg, 0.25 mg/ml). The first group was designated to evaluate PKs of rosuvastatin, carotegrast, and bromfenac, in predosed with vehicle or with RIF ($N = 3$). Blood was collected into commercially available tubes (Jiangsu Kangjian Medical Supplies Co., LTD.) containing Potassium (K2) EDTA*2H2O (0.85–1.15 mg) on wet ice at 0, 0.25, 0.5, 0.583, 0.75, 1, 1.5, 2.5, 4, 6, 8, 12, and 24 h. Blood samples were processed for plasma within 30 min of collection. An aliquot of plasma (150 µl) was transferred to amber micro-centrifuge tubes preloaded with 3 µl of formic acid (final formic acid concentration 2%). The second group was to determine liver exposure in the absence ($N = 6$) and presence ($N = 6$) of RIF. At 1, 2.5, and 6 h post the IV infusion, animals ($N = 2$ per time point) were anesthetized with IV injection of pentobarbital sodium (60 mg/kg). Aliquots (~ 1 g) were sampled from the left liver lobe and frozen immediately in liquid nitrogen. Plasma samples were also collected in a similar method for each monkey up to the time of liver sampling. All plasma and liver samples were protected from light and stored at −60°C or below until analysis.

The detailed method for sample preparation and liquid chromatography-tandem accurate mass spectrometry (LC-MS/MS) analysis to quantify rosuvastatin, carotegrast, bromfenac, CP-I, CP-III, and RIF are described in the Supplementary Material. The PK parameters of rosuvastatin, carotegrast, bromfenac, CP-I, CP-III, and RIF were derived from plasma concentrations versus time with a noncompartmental analysis (NCA) model using Phoenix software (Certara, Princeton, NJ). Statistical tests were conducted using Student's *t*-test and differences were considered significant when $p < 0.05$.

### In vitro hepatic uptake and biliary clearance

The hepatic uptake clearance of rosuvastatin, carotegrast, and bromfenac was evaluated in vitro using suspension hepatocytes as described previously with modifications.[12,18] Briefly, intracellular accumulation of test compound was determined in suspension hepatocyte incubated at 4°C and 37°C up to 5 min. The OATP activity was also assessed at 37°C in the presence of 200 µM rifamycin-SV. The hepatocytes were diluted to 2 million cells/ml in KHB with 10% (v/v) cynomolgus monkey serum. The detailed method for sample preparation and LC-MS/MS analysis are described in the Supplementary Material. The active transporter-mediated uptake was assessed at 37°C and passive diffusion was assessed at 4°C, assuming minimal transporter activities at low temperature. The total hepatic uptake and passive clearance were obtained from the initial uptake rates at 37°C or 4°C, respectively. The initial uptake rates were estimated from the slopes of linear uptake phase using linear regression analysis. Active uptake clearance was calculated by subtracting the passive uptake clearance from the total clearance. The unbound active and passive uptake clearance ($CL_{u,int,active}$, and $CL_{u,int,passive}$) were calculated by dividing the initial uptake velocity by the unbound fraction of nominal substrate concentration. The detail of calculation is described in the Supplementary Material.

In vitro biliary clearance was estimated in sandwich-cultured cynomolgus monkey hepatocytes (SCCHs). Cryopreserved monkey hepatocytes were thawed into plating medium (INVITROGRO CP, BioIVT). The cells were seeded at $4 \times 10^5$ cells per well in 24-well collagen-coated plates. After 4-h attachment, cells were washed once with cold incubation medium (INVITROGRO HI, BioIVT) and then overlaid with Matrigel (Corning, Tewksbury, MA) in incubation medium at 0.25 mg/ml on ice. The cells were then incubated overnight at 37°C in a humidified 5% CO2 incubator. Incubation media was changed every day for a total of 4 days. On day 4, hepatocytes were washed twice and preincubated for 10 min at 37°C in either HBSS buffer, or $Ca^{2+}/Mg^{2+}$-free HBSS containing 1 mM EGTA. Compounds dissolved in protein free HBSS buffer were added at final concentration of 1 μM and incubated at 37°C up to 10 min. Midazolam was used as negative control. The hepatocytes were collected in duplicate for each condition. The detailed method of LC-MS/MS quantification and the in vitro intrinsic clearance calculation are described in the Supplementary Material.

## Physiologically-based pharmacokinetic modeling

A PBPK model was built to understand the impact of OATP inhibition on the PKs of rosuvastatin, carotegrast, and bromfenac in monkeys. The PBPK model was structured using SAAM II software (the Epsilon Group, Charlottesville, VA) with 14 compartments representing major organs, including the lungs, kidneys, brain, muscles, adipose, heart, skin, bones, spleen, gut, liver, and the rest of body, which were connected by the arterial and venous circulating system (Figure S1). All organs were treated as perfusion limited compartments except for the liver, which was permeability limited. A five-compartmental liver model was adapted from previously publications.[11,12,19] Briefly, the extracellular compartment (EC) and intracellular compartment (IC) of the liver were divided equally in five compartments and every drug was cleared through each compartment in a sequential manner. A $K_p$ scalar was included in the model, which was equally applied to all predicted $K_p$ values for non-liver tissues. The $K_p$ scalar was used to optimize and improve the model to capture in vivo distribution profile. The rest of the body compartment lumping other tissues (i.e., eyes, carcass, deep tissue compartments, etc.), in addition to the organs listed above, serviced as a slow distribution organ in the model for better capturing the drug distribution profile. The differential equations describing each compartment and parameter applied in the PBPK model were included in Supplementary Methods and Table S1, respectively.

Biliary clearance was assumed to be the major route of elimination for rosuvastatin and carotegrast,[20,21] whereas metabolism in the liver was assumed to be the major pathway of elimination for bromfenac[22] in the model fitting. Urinary excretion of rosuvastatin in monkeys was reported to be ~ 20% of the absorbed dose.[12,23] In the rosuvastatin model, the renal clearance was fixed to 20% of total CL (4.4 ml/min/kg), which is comparable to the previous reported value.[23] Urinary excretion of carotegrast was estimated to be 7.5% of total dose from an in-house bile duct cannulation (BDC) monkey study (data not shown). For bromfenac, no urinary excretion was assumed. The data of plasma and liver concentration was simultaneously fitted to estimate the liver intrinsic passive uptake clearance ($CL_{u,int,passive}$), active uptake clearance ($CL_{u,int,active}$), metabolic clearance ($CL_{u,int,meta}$), or biliary excretion clearance ($CL_{u,int,bile}$), $K_p$ scalar, and the partition coefficient for the rest of the body ($K_{p,rest}$). The initial input of intrinsic $CL_{u,int,active}$, $CL_{u,int,passive}$, $CL_{u,int,meta}$, and $CL_{u,int,bile}$ in the model were scaled from the in vitro intrinsic clearance (Table S3). All of the above parameters were first estimated based on the drug profiles in the absence of RIF. The estimated $K_{p,rest}$ and $K_p$ scalar values were then fixed in the model to estimate the clearance parameters in the presence of RIF.

# RESULTS

## In vitro hepatic uptake and biliary excretion of rosuvastatin, carotegrast, and bromfenac

The uptake of rosuvastatin, carotegrast, and bromfenac in suspension monkey hepatocytes are shown in Figure 1. The intracellular accumulation of all three drugs increased in a time-dependent manner at 37°C incubation. The hepatocyte uptake was almost abolished at 4°C. In the presence of 200 μM of rifamycin SV, the uptake of rosuvastatin and carotegrast were greatly inhibited and appeared to be comparable to the uptake at 4°C. However, rifamycin SV was only able to partially inhibit the hepatocyte uptake of bromfenac. The derived in vitro CL values of hepatic uptake are summarized in Table S2.

For both rosuvastatin and carotegrast, biliary clearance is the major elimination path in humans and animals.[20] As expected, higher accumulation was shown in the buffer with $Ca^{2+}$ compared to the $Ca^{2+}$ free buffer, suggesting significant biliary excretion detected in SCCH; whereas there was no difference in the accumulation between $Ca^{2+}$ buffer and $Ca^{2+}$ free buffer for the negative control, midazolam (Figure 1d). Rosuvastatin was used as a positive control in our in-house assay and the data aligned with our historical data. As previously published, the major routes of elimination for bromfenac were glucuronidation and P450 oxidation[22]; therefore bromfenac was not assayed in SCCH.

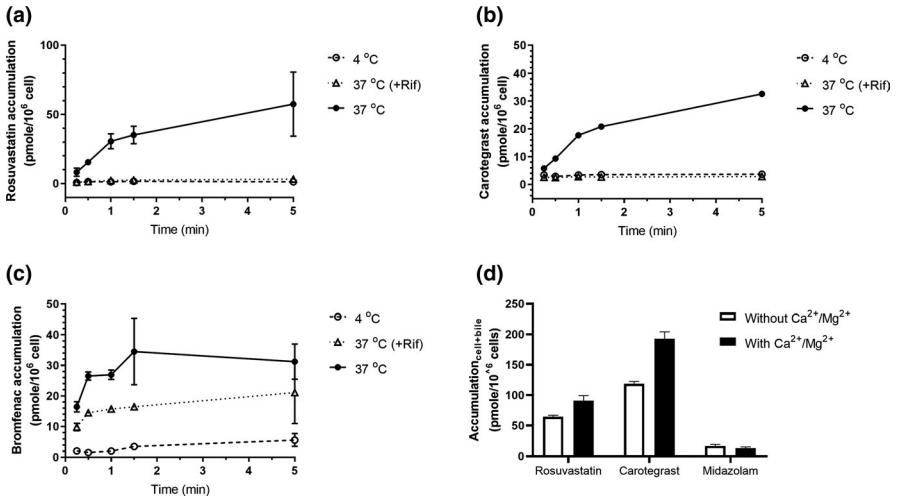


**FIGURE 1** In vitro evaluation of hepatic uptake and biliary excretion of rosuvastatin, carotegrast, and bromfenac. Intracellular accumulation of rosuvastatin (a, mean ± SD in triplicates), carotegrast (b, mean from duplicates), and bromfenac (c, mean ± SD in triplicates) in suspension hepatocytes and biliary excretion of rosuvastatin and carotegrast in sandwich-cultured cynomolgus monkey hepatocyte (SCCH), (d, mean ± SD in triplicates)

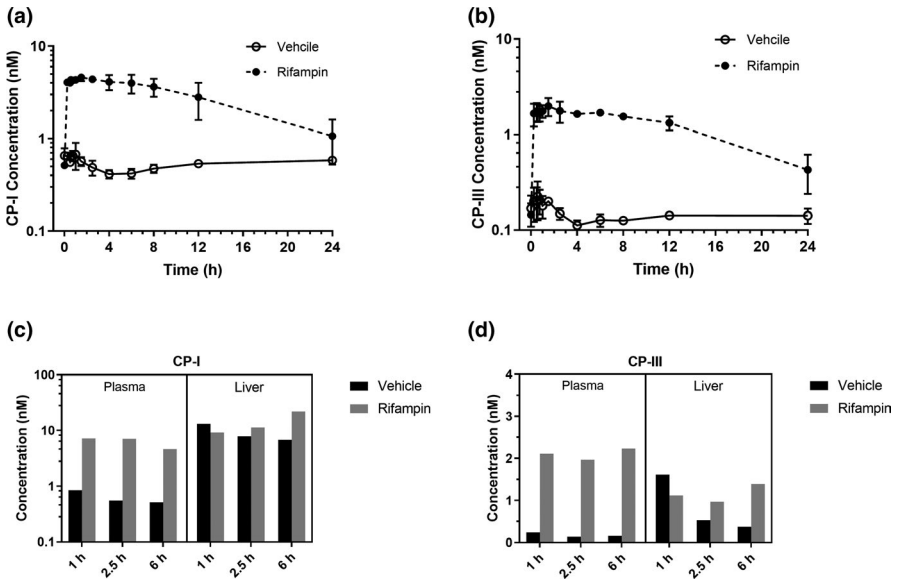


**FIGURE 2** Plasma and liver concentrations of coproporphyrin CP-I (a, c) and CP-III (b, d) in cynomolgus monkeys dosed with a single IV infusion (30 min) of three drug combination solution (0.5 mg/kg each) pretreated with oral amination of vehicle or rifampin (20 mg/kg). Plasma concentrations from group 1 (a, b) are presented as mean ± SD ($N = 3$); Comparisons between plasma and liver concentrations (c, d) at 1, 2.5, and 6 h from group 2 are presented as mean values ($N = 2$)

## Pharmacokinetic of rifampin

Following oral administration, the mean plasma concentration of RIF was 20.8 μM at 3.25 h postdosing (0.25 h post IV dose) in group 1 and group 2 (Figure S2). Time to maximum plasma concentration ($T_{max}$) was observed at 3.5–4.5 h post-RIF oral dose and the liver to plasma ratio ($K_{p,liver}$) was about 10. The plasma concentration was above 10 μM 6 h after the IV doses of OATP substrates.

## CP-I and CP-III exposure in plasma and the liver in the presence and absence of RIF

In the presence of RIF, plasma concentrations of both endogenous CP-I and CP-III were increased (Figure 2). Accordingly, the plasma exposure (area under the concentration-time curve from time of administration up to the time of the last quantifiable concentration [$AUC_{last}$]) was increased 5.4 and 8.8-fold for CP-I and CP-III, respectively (Table 1). In contrast, the liver concentration was minimally changed at 1 h but increased on average of 3.2 and 3.7-fold at 6 h for CP-I and CP-III, respectively.

## Pharmacokinetics of rosuvastatin, carotegrast, and bromfenac

In the group 1, the treatment of RIF (20 mg/kg) increased the plasma exposure of rosuvastatin, carotegrast, and bromfenac (Figure 3). The changes were the most prominent for carotegrast with maximum plasma concentration ($C_{max}$) and $AUC_{last}$ increasing 4.8 and 9.1-fold, respectively (Table 1). The CL

**TABLE 1** Pharmacokinetics of rosuvastatin, carotegrast and bromfenac following a single IV infusion (30 min) of three drug combination solution (0.5 mg/kg each) to cynomolgus monkeys pretreated with vehicle or 20 mg/kg rifampin orally ($n$ = 3, mean ± SD)

| | Rosuvastatin | | Carotegrast | | Bromfenac | | CP-I | | CP-III | |
|---|---|---|---|---|---|---|---|---|---|---|
| | Vehicle | Rifampin | Vehicle | Rifampin | Vehicle | Rifampin | Vehicle | Rifampin | Vehicle | Rifampin |
| $T_{1/2}$ (h) | 4.21 ± 0.61 | 4.63 ± 1.03 | 0.82 ± 0.51 | 1.49 ± 0.11 | 1.10 ± 0.46 | 1.14 ± 0.02 | – | – | – | – |
| Plasma CL (ml/min/kg) | 22.02 ± 1.91 | 9.96 ± 3.18* | 6.91 ± 4.00 | 0.69 ± 0.25* | 9.97 ± 1.36 | 4.72 ± 0.88* | – | – | – | – |
| V (ml/kg) | 489 ± 75 | 452 ± 210 | 114 ± 63 | 45 ± 16* | 192 ± 21 | 138 ± 31 | – | – | – | – |
| $C_{max}$ (nM) | 1598 ± 155 | 3302 ± 1061* | 4717 ± 1827 | 22806 ± 6572* | 4488 ± 696 | 8408 ± 2495* | 0.77 ± 0.15 | 4.83 ± 0.26* | 0.25 ± 0.06 | 2.03 ± 0.38* |
| $AUC_{last}$ (h*nM) | 786 ± 64 | 1842 ± 610* | 2625 ± 1209 | 23770 ± 8626* | 2522 ± 335 | 5401 ± 1087* | 12.6 ± 1.00 | 68.6 ± 18.71* | 3.38 ± 0.36 | 29.7 ± 0.95* |

Abbreviations: $AUC_{last}$, area under the concentration-time curve from time of administration up to the time of the last quantifiable concentration; CL, clearance; $C_{max}$, peak plasma concentration; CP, coproporphyrin; $T_{1/2}$, terminal half-life; V, volume.

*$p < 0.05$ as compared to the vehicle group.

of carotegrast correspondingly decreased about 10-fold in the presence of RIF, whereas the volume of distribution (V) was also reduced about a half from 0.11 to 0.05 L/kg. RIF also increased systemic exposures of rosuvastatin and bromfenac, with the $AUC_{last}$ changes of 2.3 and 2.1-fold, respectively. The systemic CLs of rosuvastatin and bromfenac were reduced by 2.2-fold, and 2.1-fold, respectively. The volume distributions of rosuvastatin and bromfenac were also reduced.

The group 2 was designed to characterize the impact of OATP inhibition on liver exposure. Although similar increases of plasma exposures for rosuvastatin, carotegrast, and bromfenac were observed by the treatment of RIF, the impact of OATP inhibition on the liver drug exposures appeared to be different. The liver concentrations overlapped at 1, 2.5, and 6 h for rosuvastatin and bromfenac between the vehicle and RIF pretreated groups (Figure 3d,f). For carotegrast, the liver concentrations were comparable at 1 h but were higher at 2.5 h and 6 h in the RIF-treated group than the vehicle group (Figure 3e and Figure S3). As shown in Figure S3, the average of $K_{p,liver}$ values were about 100, 17, and 2 for rosuvastatin, carotegrast, and bromfenac, respectively, and were reduced by the treatment of RIF.

## PBPK modeling

In order to mechanistically describe the changes of plasma and liver concentrations following the treatment of OATP inhibitor, a monkey PBPK model was constructed to incorporate the in vitro parameters to interpret in vivo monkey PK and measured liver exposure. Empirical scaling factors were assigned to compensate for the discrepancy from in vitro scaled intrinsic clearance measured in hepatocyte models to in vivo parameters yielded from curve fitting (Table S3). The observed and model fitted plasma and liver concentrations are shown in Figure 4. With scaling factors applied to the active hepatic uptake, biliary, and passive diffusion, the model reasonably described the systemic and liver concentrations of all three drugs. The reliability of in vivo parameters obtained from the curve fitting in the model was further verified by the DDI data. The model was able to accurately fit the observed plasma concentration time profile of rosuvastatin, carotegrast, and bromfenac in RIF-treated monkeys, in which the hepatic uptake clearance was reduced while the passive permeability ($CL_{,u,int,passive}$) was not changed for all three drugs. As such, the model captured the liver exposures of carotegrast and bromfenac. In contrast, the model overpredicted the liver concentration of rosuvastatin at early time points (1 and 2.5 h). The model fitted parameters and percent of the coefficients of variation (%CV) on parameter estimates are summarized in Table 2. Furthermore, the sensitivity analysis was conducted to elucidate the interplays among $CL_{u,int,passive}$, $CL_{u,int,active}$, $CL_{u,int,bile}$, or $CL_{u,int,met}$ and the plasma and live exposure. As shown in Figure S4,

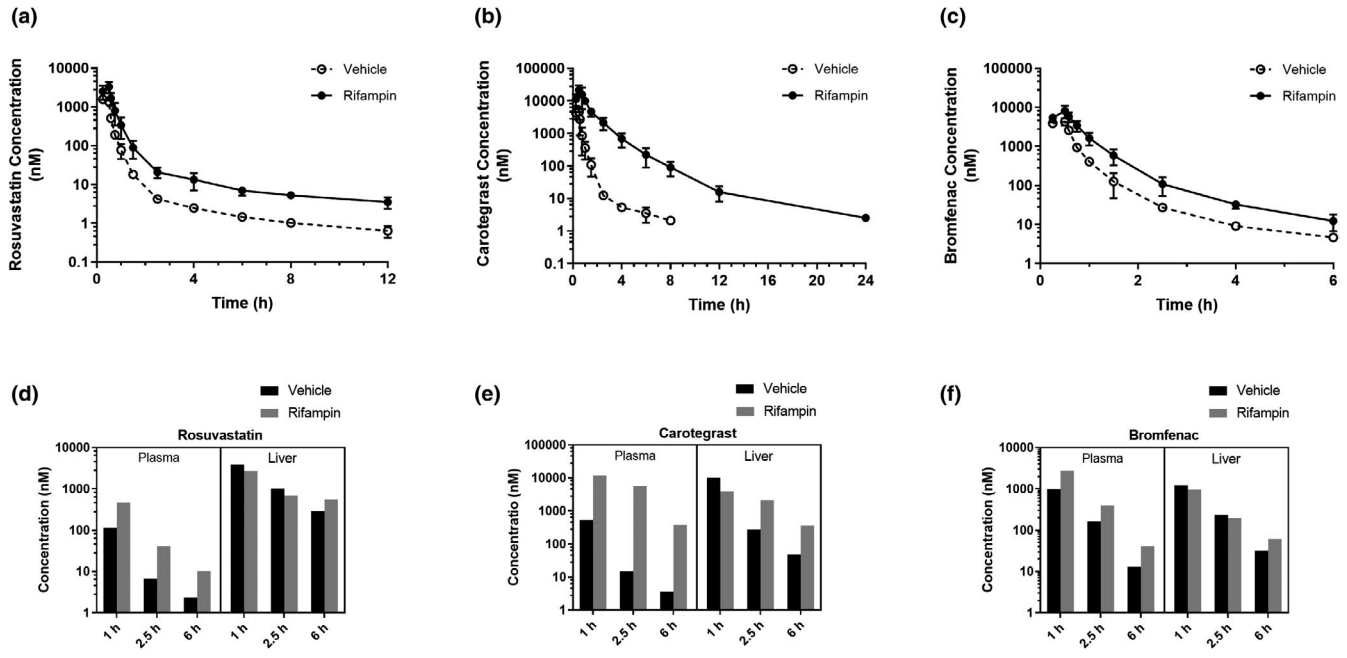


**FIGURE 3** Plasma and liver concentrations of rosuvastatin (a, d), carotegrast (b, e) and bromfenac (c, f) following a single IV infusion (30 min) of three drug combination solution (0.5 mg/kg each) in cynomolgus monkeys in the absence or presence of rifampin (20 mg/kg) oral administration. Plasma concentrations from group 1 (a, b, c) are presented as mean ± SD ($N = 3$); comparisons between plasma and liver concentrations (d, e, f) at 1, 2.5, and 6 h from group 2 are presented as mean values ($N = 2$)

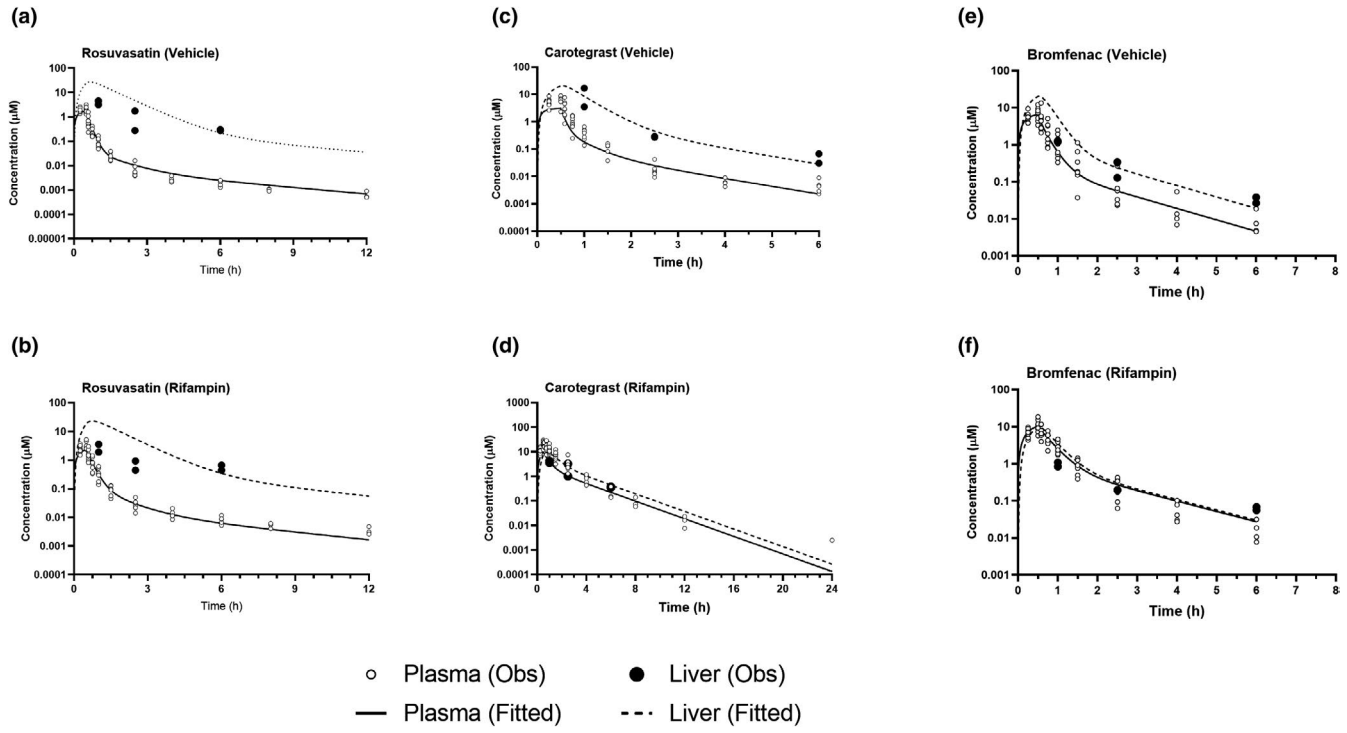


**FIGURE 4** Observed and fitted plasma and liver concentration of rosuvastatin (a, b), carotegrast (c, d), and bromfenac (e, f) in cynomolgus monkeys pretreated with oral amination of vehicle or rifampin (20 mg/kg)

generally, the $CL_{u,int,passive}$ and $CL_{u,int,active}$ are more sensitive parameters to affect plasma concentration, whereas the $CL_{u,int,bile}$ or $CL_{u,int,met}$ are more sensitive to regulate liver exposure of the three OATP substrates.

## DISCUSSION

Hepatic transport, including passive diffusion and active sinusoidal membrane transport, is a major player in systemic

**TABLE 2** Estimated parameters from plasma and liver concentrations of rosuvastatin, carotegrast, and bromfenac in cynomolgus monkeys using PBPK model

| | Rosuvastatin | | Carotegrast | | Bromfenac | |
|---|---|---|---|---|---|---|
| | Vehicle | Rifampin | Vehicle | Rifampin | Vehicle | Rifampin |
| $CL_{u,int,active}$ (ml/min/kg) | 331.8 (13.8%) | 81.7 (8.5%) | 1154.1 (5.2%) | 95.2 (4.4%) | 2300 (18.7%) | 820 (10.8%) |
| $CL_{,u,int,passive}$ (ml/min/kg) | 1.0 (22.5%) | 0.5 (41%) | 4.1(11.8%) | 2.9 (32.4%) | 13.1 (96.2%) | 11.2 (95.3%) |
| $CL_{u,int,bile}$ (ml/min/kg) | 2.8 (1.7%) | 2.6 (19.7%) | 16.3 (0.022%) | 11.7 (0.1%) | NA | NA |
| $CL_{u,int,meta}$ (ml/min/kg) | NA | NA | NA | NA | 49.7 (16.9%) | 84.8 (3.8%) |
| $K_{p,rest}$ | 2.7 (4.5%) | 2.7 (fixed) | 0.85 (6.1%) | 0.85 (fixed) | 0.8 (6.3%) | 0.8 (fixed) |
| $K_{p,scalar}$ | 1.1 (3.5%) | 1.1 (fixed) | 0.16 (29.4%) | 0.16 (fixed) | 0.5 (27%) | 0.5 (fixed) |
| V (ml/kg) | 394 | 404 | 132 | 116 | 121 | 114 |
| CL (ml/min/kg) | 18.3 | 11.7 | 8.3 | 1.2 | 6.7 | 3.3 |

Plasma from two groups of animals ($n = 9$) and liver concentrations ($n = 2$ per time point) were simultaneously fitted to estimate parameters and the coefficients of variation (%CV). All of the above parameters were first estimated in the absence of rifampin. The estimated $K_{p,rest}$ and $K_p$ scalar values were then applied in the model to estimate the clearance parameters in the presence of rifampin. The V and CL were calculated from simulated plasma PK with a noncompartmental model (NCA).

Abbreviations: $CL_{u,int,bile}$, intrinsic biliary excretion clearance; $CL_{u,int,active}$, intrinsic active uptake clearance; $CL_{u,int,meta}$, intrinsic metabolic clearance; $CL_{,u,int,passive}$, intrinsic passive uptake clearance; NA, not applicable; PBPK, physiologically-based pharmacokinetic.

clearance of a drug, and more importantly controls drug availability for the metabolism and biliary clearance in the liver. Although the passive permeation is a compound-dependent parameter that relates to physiochemical properties, such as logD and pKa, etc., active hepatic uptake is attributed to membrane transporter(s) expressed on the sinusoid membrane of hepatocytes. On many occasions, the active uptake can be attributed by more than one transporter due to the overlapping of substrate specificity. Therefore, three drugs with different chemotype and metabolic/excretion profiles were studied here to comprehensively evaluate the impact of reduction of OATP activity on their plasma PK and liver exposures in cynomolgus monkeys. In addition, the changes followed by the administration of the OATP inhibitor RIF offer the best case to construct a PBPK model to understand interplays among hepatic uptake, metabolism, and biliary excretions.

Rosuvastatin, bromfenac, and carotegrast are all known to be OATP substrates but have different elimination profiles on metabolism and additional transporter-mediated uptake and biliary efflux. All three OATP transporters (OATP1B1, 1B3, and 2B1) in the liver are known to contribute to the liver uptake of rosuvastatin.[24] Rosuvastatin is mainly cleared in the bile as the parent drug, with less than 10% cleared through renal excretion in humans.[25] Bromfenac is a nonsteroidal anti-inflammatory drug, which is a substrate for both OATPs and OAT2.[26,27] Bromfenac is mainly eliminated by hepatic biotransformation via a combination of oxidative and conjugative mechanisms as bromfenac glucuronide is excreted in urine and accounts for 82.5% of the administered dose in healthy subjects.[28] Carotegrast, a parent drug of carotegrast methyl developed for the treatment of active ulcerative colitis, is a substrate for OATP1B1 and OATP1B3.[20] Carotegrast is minimally excreted in urine but primarily eliminated in bile via MRP2 in humans.[20] The results observed in the suspension hepatocyte uptake assays are in good agreement with the above literature publications. In vitro hepatocyte uptake of rosuvastatin and carotegrast were almost abolished by 200 μM rifamycin SV in the current study, which is much higher than the reported $K_i$ values of 2 and 3 μM against OATP1B1 and OATP1B3, respectively.[29] On the other hand, the uptake of bromfenac was only partially inhibited by rifampicin SV. This is consistent with earlier report that the half-maximal inhibitory concentration ($IC_{50}$) of rifamycin SV for OAT2 was around 200 μM,[27] and the OAT2 activity was not fully inhibited by rifamycin SV in the current assay condition.

The impact of OATP inhibition on plasma and liver exposures was investigated in monkeys receiving a single IV cassette dose of rosuvastatin, bromfenac, and carotegrast at 0.5 mg/kg each. The selection of cassette dosing was to minimize the animal use and intersubject variations. The plasma exposure (AUC) of rosuvastatin, when normalizing to the dose, and the OATP biomarkers CP-I and CP-III in the presence and absence of rifampin in our study were consistent with literature data reported in monkeys,[5,6,16] therefore the data confirmed the lack of interactions among these three compounds in a cassette dose. In addition, the large change of plasma AUC in CP-III can be due to an additive effect of hepatic and renal CL inhibition of CP-III, as reported by

Shen et al.[5] Although urine sample collection was included in the study design, no meaningful urine excretion data were obtained probably due to sample handling errors. A previous study showed that RIF increased the amount of rosuvastatin excreted in urine due to increase plasma exposure, but the renal CL remains unchanged.[23]

The exposure of RIF dosed at 20 mg/kg in the monkeys was above the threshold of OATP inhibition (Figure S2). Therefore, it is expected that the plasma exposures of rosuvastatin, bromfenac, and carotegrast would increase followed by RIF treatment, although the magnitudes of AUC change are different among the three drugs. Although rifamycin SV fully inhibited hepatic uptake of rosuvastatin in hepatocytes in vitro, RIF treatment only increased rosuvastatin AUC about twofold. One of the explanations is that the clearance of rosuvastatin in monkeys was close to liver blood flow, and thus, the CL of rosuvastatin could be hepatic blood flow-limited when dosed intravenously.[16] Additionally, rosuvastatin is a substrate of monkey NTCP,[17,30] and under the in vitro condition with high concentration of rifamycin SV, the NTCP-mediated active uptake can be inhibited. The disconnection of in vitro OATP inhibition to in vivo observation likely reflected the contribution of NTCP to rosuvastatin uptake that was not fully inhibited by RIF in vivo. For bromfenac, an approximately twofold AUC increase was also observed in monkeys treated with rifampicin. The smaller DDI could be due to the involvement of OAT2, which is not inhibited by rifampin in the current study.[27] In contrast, AUC increased more extensively with OATP inhibition for carotegrast, indicating that OATP-mediated transport could be the predominant contributor to the hepatic uptake clearance.

The impacts of RIF inhibition on liver concentrations were different when compared with plasma exposures. The $K_{p,liver}$ was decreased for all three drugs by the treatment of RIF, but the liver concentrations were not reduced. With incorporation of in vitro clearances obtained from hepatocyte assays, the monkey PBPK model was able to simultaneously fit the exposures of plasma and liver in the presence and absence of OATP inhibitor, RIF. Consistent with literature reports, scaling factors are needed to translate parameter values from in vitro to in vivo.[12,19] Based on the PBPK model, both passive permeability and OATP-mediated active uptake, as well as the involvement of other transporters, determine the $K_{p,liver}$. A reduction of 75% was modeled for rosuvastatin active uptake clearance with rifampin inhibition. The average $K_{p,liver}$ of rosuvastatin in the presence of rifampin was still greater than 1, suggesting that other transporters (e.g., NTCP) can also contribute to the liver uptake in monkeys. The active uptake of bromfenac was only reduced by 64% with RIF inhibition, consistent with the observation in suspension hepatocytes. Given the extensive metabolism of bromfenac, the influence of RIF on its metabolic clearance and biliary excretion are negligible, and therefore the unchanged liver concentration is due to passive permeability and OAT2 activity. Interestingly, the model analysis suggested that biliary excretion of carotegrast was reduced slightly in the presence of RIF while passive permeability remained unchanged, leading to the liver accumulation. Carotegrast was determined to be a substrate of MRP2 in vitro (unpublished in-house data). Similar profiles were also observed for CP-I and CP-III, which were also reported to be MRP2 substrates.[31] Previous studies suggested that RIF could inhibit MRP2 in addition to OATPs in humans.[32,33] As shown in Figure S4, the sensitivity analysis suggested that both hepatic uptake inhibition and impaired monkey MPR2 activity by rifampin treatment can partially explain the higher liver exposure of carotegrast, CP-I, and CP-III. Aligned with the above discussions, the model sensitivity analysis confirmed that the active uptake clearance was the key factor contributing to the plasma exposure, whereas the metabolism or biliary excretion was critical for regulating liver concentration. One of the limitations of the current PBPK model was that it does not incorporate the enterohepatic circulation (EHC). In humans, rosuvastatin has a long terminal half-life resulting from EHC.[34] In the current study, the plasma concentrations were able to detect up to 12 h in monkeys. The EHC unlikely occurred for carotegrast as it has low intestinal absorption and therefore is dosed as prodrug to boost the absorption.[20] Therefore, the EHC component may have minimal impact on the current PBPK modeling.

Overall, inhibition of OATP activity increased systemic exposure and reduced the liver to plasma ratio of all three drugs, but the liver exposure of the drugs remained unchanged. Our findings of rosuvastatin in monkeys agree with the earlier report that total radioactivity of $^{11}$C-rosuvastatin was not significantly changed in the human liver in the first 30 min with OATP function attenuated.[13] Because we were able to quantify the rosuvastatin in plasma and the liver for up to 6 h, rather than the total radioactivity (rosuvastatin and its metabolites), which allowed us to construct the PBPK model to understand the interactions among liver OATP uptake, biliary excretion and metabolism based on observed data. In addition, a recent clinical trial data indirectly supported our findings and modeling analysis in monkeys. The pharmacodynamic (PD) effect of GS-0976, a liver-targeted ACC inhibitor under clinical development, was not altered by potent OATP inhibitor, although its plasma concentration was increased significantly.[35] Most likely the liver exposure of GS-0976 was not changed by OATP inhibition. Extending this finding to the liver disease population, such as nonalcoholic fatty liver disease[36] and patients with genetic variants in hepatic transporters, the transporter function can be reduced; however, the liver drug exposure may not be affected in these populations. Understanding factors that regulate the liver drug exposure is critical to estimate the efficacious dose in patients, especially for liver-targeting therapeutic reagents. It should be

noted that OATPs are only one class of transporters in the liver, and there are many other transporters expressed on the sinusoidal and canalicular membrane of hepatocytes. When other extrahepatic CL pathways playing a significant role in overall CL, the inhibition of hepatic uptake (e.g., OATP inhibition) can result in the reduction of liver exposure, which had been showed in the model simulation by Patilea-Vrana et al.[37] Therefore, it is important to consider all these factors together to understand the tissue exposure of a drug in various clinical scenarios. More importantly, species differences regarding the function of OATP and other transporters between monkeys and humans must be noted and the drug metabolic profiles could also be different. Further investigations are necessary to translate the current observations to humans.

To the best of our knowledge, this is the first study evaluating the impact of OATP inhibition on the plasma and liver exposure of three OATP substrates with distinct elimination routes and PK profiles in monkeys. The study demonstrates that inhibition of OATP activities can increase the plasma exposure of OATP substrates but have minimum impact on liver drug exposure in monkeys. The PBPK model using in vitro parameters in combination with scaling factors is a viable approach to model the interplay of in vivo processes of hepatic transport, drug metabolism, and biliary excretion, and elucidate the differential changes of plasma and liver concentrations.

## CONFLICT OF INTEREST

All authors were employees of Gilead Sciences Inc. during this research.

## AUTHOR CONTRIBUTIONS

Y.C., X.L., and Y.L. wrote the manuscript. Y.C., and Y.L. designed the research. X.L., J.H., and C.N. performed the research. Y.C., X.L., J.H., C.N., and Y.L. analyzed the data.

## REFERENCES


1. Mikkaichi T, Suzuki T, Tanemoto M, Ito S, Abe T. The organic anion transporter (OATP) family. *Drug Metab Pharmacokinet*. 2004;19:171-179.
2. van de Steeg E, Stránecký V, Hartmannová H, et al. Complete OATP1B1 and OATP1B3 deficiency causes human Rotor syndrome by interrupting conjugated bilirubin reuptake into the liver. *J Clin Invest*. 2012;122:519-528.
3. Slijepcevic D, Roscam Abbing RLP, Katafuchi T, et al. Hepatic uptake of conjugated bile acids is mediated by both sodium taurocholate cotransporting polypeptide and organic anion transporting polypeptides and modulated by intestinal sensing of plasma bile acid levels in mice. *Hepatology*. 2017;66:1631-1643.
4. Suga T, Yamaguchi H, Sato T, Maekawa M, Goto J, Mano N. Preference of conjugated bile acids over unconjugated bile acids as substrates for OATP1B1 and OATP1B3. *PLoS One*. 2017;12:e0169719.
5. Shen H, Dai J, Liu T, et al. Coproporphyrins I and III as functional markers of OATP1B activity. In vitro and in vivo evaluation in preclinical species. *J Pharmacol Exp Ther*. 2016;357:382-393.
6. Lai Y, Mandlekar S, Shen H, et al. Coproporphyrins in plasma and urine can be appropriate clinical biomarkers to recapitulate drug-drug interactions mediated by organic anion transporting polypeptide inhibition. *J Pharmacol Exp Ther*. 2016;358:397-404.
7. International Transporter Consortium, Giacomini KM, Huang S-M, et al. Membrane transporters in drug development. *Nat Rev Drug Discov*. 2010;9:215-236.
8. Nakanishi T, Tamai I. Genetic polymorphisms of OATP transporters and their impact on intestinal absorption and hepatic disposition of drugs. *Drug Metab Pharmacokinet*. 2012;27:106-121.
9. Prueksaritanont T, Chu X, Evers R, et al. Pitavastatin is a more sensitive and selective organic anion-transporting polypeptide 1B clinical probe than rosuvastatin. *Br J Clin Pharmacol*. 2014;78:587-598.
10. Shitara Y. Clinical importance of OATP1B1 and OATP1B3 in drug-drug interactions. *Drug Metab Pharmacokinet*. 2011;26:220-227.
11. Watanabe T, Kusuhara H, Maeda K, Shitara Y, Sugiyama Y. Physiologically based pharmacokinetic modeling to predict transporter-mediated clearance and distribution of pravastatin in humans. *J Pharmacol Exp Ther*. 2009;328:652-662.
12. Morse BL, MacGuire JG, Marino AM, et al. Physiologically based pharmacokinetic modeling of transporter-mediated hepatic clearance and liver partitioning of OATP and OCT substrates in cynomolgus monkeys. *AAPS J*. 2017;19:1878-1889.
13. Billington S, Shoner S, Lee S, et al. Positron emission tomography imaging of [(11) C]Rosuvastatin hepatic concentrations and hepatobiliary transport in humans in the absence and presence of cyclosporin A. *Clin Pharmacol Ther*. 2019;106:1056-1066.
14. Shen H, Yang Z, Mintier G, et al. Cynomolgus monkey as a potential model to assess drug interactions involving hepatic organic anion transporting polypeptides: in vitro, in vivo, and in vitro-to-in vivo extrapolation. *J Pharmacol Exp Ther*. 2013;344:673-685.
15. Takahashi T, Uno Y, Yamazaki H, Kume T. Functional characterization for polymorphic organic anion transporting polypeptides (OATP/SLCO1B1, 1B3, 2B1) of monkeys recombinantly expressed with various OATP probes. *Biopharm Drug Dispos*. 2019;40:62-69.
16. Chu X, Shih S-J, Shaw R, et al. Evaluation of cynomolgus monkeys for the identification of endogenous biomarkers for hepatic transporter inhibition and as a translatable model to predict pharmacokinetic interactions with statins in humans. *Drug Metab Dispos*. 2015;43:851-863.
17. Shen H, Su H, Liu T, et al. Evaluation of rosuvastatin as an organic anion transporting polypeptide (OATP) probe substrate: in vitro transport and in vivo disposition in cynomolgus monkeys. *J Pharmacol Exp Ther*. 2015;353:380-391.
18. Liang X, Park Y, DeForest N, et al. In vitro hepatic uptake in human and monkey hepatocytes in the presence and absence of serum protein and its in vitro to in vivo extrapolation. *Drug Metab Dispos*. 2020;48:1283-1292.
19. Jones HM, Barton HA, Lai Y, et al. Mechanistic pharmacokinetic modeling for the prediction of transporter-mediated disposition in humans from sandwich culture human hepatocyte data. *Drug Metab Dispos*. 2012;40:1007-1017.
20. Fukase H, Kajioka T, Oikawa I, Ikeda N, Furuie H. AJM300, a novel oral antagonist of alpha4-integrin, sustains an increase in

circulating lymphocytes: A randomised controlled trial in healthy male subjects. *Br J Clin Pharmacol.* 2020;86:591-600.
21. Kimoto E, Bi YA, Kosa RE, Tremaine LM, Varma MVS. Hepatobiliary clearance prediction: species scaling from monkey, dog, and rat, and in vitro-in vivo extrapolation of sandwich-cultured human hepatocytes using 17 drugs. *J Pharm Sci*. 2017;106:2795-2804.
22. Driscoll JP, Yadav AS, Shah NR. Role of glucuronidation and P450 oxidation in the bioactivation of bromfenac. *Chem Res Toxicol*. 2018;31:223-230.
23. Kosa RE, Lazzaro S, Bi Y-A, et al. Simultaneous assessment of transporter-mediated drug-drug interactions using a probe drug cocktail in cynomolgus monkey. *Drug Metab Dispos*. 2018;46:1179-1189.
24. Ho R, Wang Y, Leake B, Kim R. Multiple OATP transporters mediate the cellular uptake of rosuvastatin. *Clin Pharmacol Ther.* 2005;77:64.
25. Martin PD, Warwick MJ, Dane AL, et al. Metabolism, excretion, and pharmacokinetics of rosuvastatin in healthy adult male volunteers. *Clin Ther*. 2003;25:2822-2835.
26. Kimoto E, Mathialagan S, Tylaska L, et al. Organic anion transporter 2-mediated hepatic uptake contributes to the clearance of high-permeability-low-molecular-weight acid and zwitterion drugs: evaluation using 25 drugs. *J Pharmacol Exp Ther*. 2018;367:322-334.
27. Bi YA, Costales C, Mathialagan S, et al. Quantitative contribution of six major transporters to the hepatic uptake of drugs: "SLC-phenotyping" using primary human hepatocytes. *J Pharmacol Exp Ther*. 2019;370:72-83.
28. Skjodt NM, Davies NM. Clinical pharmacokinetics and pharmacodynamics of bromfenac. *Clin Pharmacokinet*. 1999;36:399-408.
29. Vavricka SR, Van Montfoort J, Ha HR, Meier PJ, Fattinger K. Interactions of rifamycin SV and rifampicin with organic anion uptake systems of human liver. *Hepatology*. 2002;36:164-172.
30. Bi YA, Qiu X, Rotter CJ, et al. Quantitative assessment of the contribution of sodium-dependent taurocholate co-transporting polypeptide (NTCP) to the hepatic uptake of rosuvastatin, pitavastatin and fluvastatin. *Biopharm Drug Dispos*. 2013;34:452-461.
31. Kunze A, Ediage EN, Dillen L, Monshouwer M, Snoeys J. Clinical investigation of coproporphyrins as sensitive biomarkers to predict mild to strong OATP1B-mediated drug-drug interactions. *Clin Pharmacokinet*. 2018;57:1559-1570.
32. Yoshikado T, Toshimoto K, Maeda K, et al. PBPK modeling of coproporphyrin I as an endogenous biomarker for drug interactions involving inhibition of hepatic OATP1B1 and OATP1B3. *CPT Pharmacometrics Syst Pharmacol*. 2018;7:739-747.
33. Takashima T, Kitamura S, Wada Y, et al. PET imaging-based evaluation of hepatobiliary transport in humans with (15R)-11C-TIC-Me. *J Nucl Med*. 2012;53:741-748.
34. Martin PD, Warwick MJ, Dane AL, Brindley C, Short T. Absolute oral bioavailability of rosuvastatin in healthy white adult male volunteers. *Clin Ther*. 2003;25:2553-2563.
35. Kirby BJ, Lutz JD, Garrison KL, et al. Alteration of hepatic OATP activity does not alter the pharmacodynamic effect of GS-0976, a liver-targeted ACC inhibitor, on de novo lipogenesis. 20th International Workshop on Clinical Pharmacology of HIV Hepatitis & Other Antiviral Drugs. (2019).
36. Fisher CD, Lickteig AJ, Augustine LM, et al. Experimental non-alcoholic fatty liver disease results in decreased hepatic uptake transporter expression and function in rats. *Eur J Pharmacol*. 2009;613:119-127.
37. Patilea-Vrana G, Unadkat JD. Transport vs. metabolism: what determines the pharmacokinetics and pharmacodynamics of drugs? Insights from the extended clearance model. *Clin Pharmacol Ther*. 2016;100:413-418.

## SUPPORTING INFORMATION

Additional supporting information may be found online in the Supporting Information section.

**How to cite this article:** Cheng Y, Liang X, Hao J, Niu C, Lai Y. Application of a PBPK model to elucidate the changes of systemic and liver exposures for rosuvastatin, carotegrast, and bromfenac followed by OATP inhibition in monkeys. *Clin Transl Sci*. 2021;14:1924–1934. https://doi.org/10.1111/cts.13047